https://doi.org/10.5194/hess-2020-111
Preprint. Discussion started: 25 March 2020

Hydrology and Earth System Sciences
Discussions

Flexible vector-based spatial configurations in land models

Shervan Gharari[1,*], Martyn P. Clark[1], Naoki Mizukami[2], Wouter J. M. Knoben[1], Jefferson S. Wong[3], Alain Pietroniro[4]

1- University of Saskatchewan Coldwater Laboratory, Canmore, Alberta, Canada.
2- National Center for Atmospheric Research, Boulder, Colorado, USA.
3- Global Institute for Water Security (GIWS), Saskatoon, Saskatchewan, Canada.
4- Environment and Climate Change Canada (ECCC), Saskatoon, Saskatchewan, Canada.
*Corresponding author Shervan Gharari, shervan.gharari@usask.ca

Abstract. Land models are increasingly used in terrestrial hydrology due to their process-oriented representation of water and energy fluxes. Land models can be set up at a range of spatial configurations, often ranging from grid sizes of 0.02 to 2 degrees (approximately 2 to 200 km) and applied at sub-daily temporal resolutions for simulation of energy fluxes. A priori specification of the grid size of the land models typically is derived from forcing resolutions, modeling objectives, available geo-spatial data and computational resources. Typically, the choice of model configuration and grid size is based on modeling convenience and is rarely examined for adequate physical representation in the context of modeling. The variability of the inputs and parameters, forcings, soil types, and vegetation covers, are masked or aggregated based on the a priori chosen grid size. In this study, we propose an alternative to directly set up a land model based on the concept of Group Response Unit (GRU). Each GRU is a unique combination of land cover, soil type, and other desired geographical features that has hydrological significance, such as elevation zone, slope, and aspect. Computational units are defined as GRUs that are forced at a specific forcing resolution; therefore, each computational unit has a unique combination of specific geo-spatial data and forcings. We set up the Variable Infiltration Capacity (VIC) model, based on the GRU concept (VIC-GRU). Utilizing this model setup and its advantages we try to answer the following questions: (1) how well a model configuration simulates an output variable, such as streamflow, for range of computational units,

https://doi.org/10.5194/hess-2020-111
Preprint. Discussion started: 25 March 2020

(2) how well a model configuration with fewer computational units, coarser forcing resolution and less geo-spatial information, reproduces a model set up with more computational units, finer forcing resolution and more geo-spatial information, and finally (3) how uncertain the model structure and parameters are for the land model. Our results, although case dependent, show that the models may similarly reproduce output with a lower number of computational units in the context of modeling (streamflow for example). Our results also show that a model configuration with a lower number of computational units may reproduce the simulations from a model configuration with more computational units. Similarly, this can assist faster parameter identification and model diagnostic suites, such as sensitivity and uncertainty, on a less computationally expensive model setup. Finally, we encourage the land model community to adopt flexible approaches that will provide a better understanding of accuracy-performance tradeoff in land models.

1 Introduction

Land models have evolved considerably over the past few decades. Initially, land models (or land-surface models) were developed to provide the lower boundary conditions for atmospheric models (Manabe, 1969). Since then land models have increased in complexity, and they now include a variety of hydrological, biogeophysical, and biogeochemical processes (Pitman, 2003). Including this broad suite of terrestrial processes makes land models suitable to simulate energy and water fluxes and carbon and nitrogen cycles.

Despite the recent advancements in process representation in land models, there is currently limited understanding of the appropriate spatial complexity that is justified based on the available data and the purpose of the modelling exercise (Hrachowitz and Clark, 2017). The increase of computational power, along with the existence of more accurate digital elevation models and land cover maps, encourage modellers to configure their models at the finest spatial resolution possible. Such hyper-resolution implementation of land models (Wood et al., 2011) can provide detailed simulations at spatial scales as small as 1-km^2 grid over large geographical domains (e.g., Maxwell et al., 2015). However, the computational expense for hyper-resolution models could potentially be reduced using more creative spatial discretization strategies (Clark et al., 2017).

https://doi.org/10.5194/hess-2020-111
Preprint. Discussion started: 25 March 2020

It is common to adopt concepts of hydrological similarity to reduce computational costs. In this approach, spatial units are defined based on similarity in geospatial data, under the assumption that processes, and therefore parameters, are similar for areas within a spatial unit (e.g., Vivoni et al., 2004). Hydrological Response Units (HRUs) are perhaps the most well-known technique to group geospatial attributes in hydrological models. HRUs can be built based on various geospatial characteristics; for example, Kirkby and Weyman 1974, Knudsen and Refsgaard (1986), Flügel (1995), Winter (2001), and Savenije (2010) all have proposed to use geospatial indices to discretize a catchment into hydrological units with distinct hydrological behaviour. HRUs can be built based on soil type such as proposed by Kim and van de Giessen (2004). HRUs can also be built based on fieldwork and expert knowledge (Naef et al., 2002, Uhlenbrook 2001), although the spatial domain of such classification will be limited to the catchment of interest and the spatial extent of the field measurements. HRUs are often constructed by GIS-based overlaying of various maps of different characteristics and can have various shapes such as for non-regular (sub-basins), grid, hexagon, or triangulated irregular network also known as TIN (Beven 2001, Marsh et al., 2012, Oliviera et al., 2006, Pietroniro et al., 2007). Similar approaches are used in land models. Traditionally land models use the tiling scheme where a grid box is subdivided into several tiles of unique land cover, each described as a percentage of the grid (Koster and Suarez, 1992). Land models are also beginning to adopt concepts of hydrological similarity (e.g., Newman et al., 2014; Chaney et al., 2018).

A long-standing challenge is understanding the impact of grid size on model simulations (Wood et al., 1988). The effect of model grid size can have a significant impact on model simulation across scale especially if the model parameters are linked to characteristics which are averaged out across scale (Bloschl et al., 1995). Shrestha et al. (2015) have investigated the performance of CLM v4.0 coupled with ParFlow across various grid sizes. They concluded the grid size changes of more than 100 meters can significantly affect the sensible heat and latent heat fluxes as well as soil moisture. Also using CLM, Singh et al. (2015) demonstrated that topography has a substantial impact on model simulations at the hillslope scale (~100 meters), as aggregating the topographical data changes the runoff generation mechanisms. This is understandable as the CLM is based on topographical wetness index (Beven and Kirkby 1979, Niu et al., 2005). However, Melsen et al. (2016) evaluated the transferability of parameters sets across the temporal and spatial resolutions for the Variable Infiltration Capacity (VIC) model implemented in an Alpine region. They concluded that parameter sets are more transferable across various grid sizes in comparison with parameter transferability across different temporal resolutions. Haddeland et al. (2002) showed that the transpiration from the VIC model highly depends on grid resolution. It remains debatable how model parameters and performance can vary across various grid resolutions (Liang et al., 2004; Troy et al., 2008; Samaniego et al., 2017).

The representation of spatial heterogeneity is an ongoing debate in the land modelling community (Clark et al., 2015). The key issue is to define which processes are represented explicitly and which processes are parameterized. The effect of spatial scale on emergent behaviour has been studied for catchment scale models – the concepts of Representative Elementary Areas (REA), or Representative Elementary Watersheds (REW), were introduced to study the effect of spatial aggregation on system-scale emergent behaviour (Wood et al., 1995, Reggiani et al., 1999). The effect of scale on model simulations is not well explored for land models. More work is needed to understand the extent to which the heterogeneity of process representations is sufficient for the purpose of a given modelling application, and the extent to which the existing data can support the model configurations (Wood et al., 2011, Beven et al., 2015).

In addition to the choice on model's spatial configurations, more work is needed to define the appropriate structure of land models. While many studies in hydrology have evaluated how model structure affects the smaller scale watershed response (Son and Sivapalan 2007, Clark et al., 2008, Fenicia et al., 2011, Shafii et al., 2017), this issue has received limited attention in the land modelling community (Desborough, 1999). Only recently, a few land models enable changing the process formulations within a limited range of model structural assumptions (Noah-MP, Niu et al., 2011, SUMMA, Clark et al., 2015) We explore effects of different choices of runoff generation process representation in the model.

In this study, we configure the Variable Infiltration Capacity (VIC) model in a flexible vector-based framework to understand how model simulations depend on the spatial configuration. The remainder of this paper is organized as follows: In Section 2, we present the VIC model, its vector-based implementation, and its coupling to the mizuRoute routing model. In Section 3 we describe the design of the experiments. In Section 4 we describe the results of the experiments. Section 5 discusses the implication of spatial discretization strategies on large-scale land model applications. The paper ends in Section 6 with conclusions of this study and implications for future work.

2 Land model and the routing model

2.1 The Variable Infiltration Capacity (VIC) model

The VIC model was developed as a simple land surface/hydrological model (Liang et al. 1994) that has received applications worldwide (Melsen et al., 2016). In this study we use classic VIC version 5 (VIC-5, Hamman et al., 2018). The key features of VIC are: (i) traditionally, the VIC model (version 4 and earlier) simulates sub-daily energy variables with daily forcing of minimum and maximum temperature, precipitation and wind speed. This enables the VIC model to be easily forced with hydrological available data sets worldwide while being able to solve the energy fluxes over sub-daily time periods. (ii) The VIC model combines sub-grid probability distributions to simulate surface hydrology such as variable infiltration capacity formulation (Zhao, 1982) with bio-physical formulations for transpiration (Jarvis et al., 1976).

The VIC model uses three soil layers to represent the subsurface. While each soil layer can have various physical soil parameters (e.g., saturated hydraulic conductivity, bulk density), each layer is assumed to be uniform across the entire grid regardless of the vegetation type variability in that grid. The VIC model assumes a tile vegetation implementation within each grid similar to the mosaic approach of Koster and Suarez (1992). To account for spatial variability in vegetation, the VIC model allows for root depths to be adjusted for every vegetation type. The vegetation parameters (e.g., stomatal resistance, LAI, albedo) are fixed for every land cover. The VIC model can account for different elevation zones to account for temperature lapse rate given elevation difference in a grid cell, and also for the distribution of precipitation over various elevation zones.

2.2 The VIC-GRU implementation: a vector-based configuration for land models

The VIC model is typically applied at regular grid. Figure-1a illustrates the typical VIC configuration – here the modeler selects a cell size, and then the soil, vegetation and forcing files are all aggregated or disaggregated to the target cell size. Original data resolution and spatial distribution of soil, land cover and forcing data are lost. In this study, we configure the VIC model

https://doi.org/10.5194/hess-2020-111
Preprint. Discussion started: 25 March 2020

Hydrology and Earth System Sciences Discussions

using non-regular shapes, Grouped response Units (GRUs, Kouwen et al., 1993), depending on the soil, vegetation, and topography. The GRUs hence describe unique characteristics of soil, vegetation type, elevation, slope and aspect. Figure-1b presents an example of irregular GRUs created through spatial intersections of the land use and soil types. These GRUs then can be forced at the original resolution of forcing, or upscaled or downscaled values. Computational units can then be constructed that intersect the GRUs with the forcing grid. Therefore, each computational unit has unique geospatial data such as soil, vegetation, slope and aspect and is forced with a unique forcing (a specific GRU forced with unique forcing).

The benefits of vector-based implementation of the VIC model based on the concept of GRU can be summarized as follows:

1- No grid and no assumption on grid size; *Model resolution loses it meaning*. In traditional VIC implementation, the modeler selects a grid resolution (which is often a regular latitude/longitude grid). The soil parameters and forcing data from any resolution must be aggregated, disaggregated, resampled or interpolated for every grid size. The land cover data is only considered as a percentage for every grid and spatial location of the land cover is lost. However in the VIC-GRU setup these decisions are only based on the input and forcing data that are chosen to be used in the modeling practice and no upscaling or downscaling to grid size is needed.

2- The GRUs at the resolution of the forcing data logically represent the heterogeneity of the input data (meteorological forcing and geospatial information). A higher number of computational units than the proposed setup will arguably provide an unnecessary computational burden due to identical forcing data and geospatial information.

3- Direct simplification of geospatial data. The vector-based implementation makes the direct aggregation of GRUs based on merging the geospatial data. It is easier to aggregate similar soil types or similar forested areas into a unified GRU with basic GIS function (dissolving for example) than this would be if all data had to be converted to a uniform grid first.

4- Direct specification of physical parameters. As each of the GRUs have specific type of land cover, soil type and other physical characteristics, it is straightforward to specify parameter

https://doi.org/10.5194/hess-2020-111
Preprint. Discussion started: 25 March 2020

values based on look up tables (i.e., no averaging, upscaling or smearing is needed). This is favorable because the modeler does not need to make decisions about methods used for upscaling of geophysical data at the grid level.

5- The ability to compare and constrain the parameter values for GRUs and their simulations. The impact of land cover, soil type and elevation zone can be evaluated separately. For example, the GRU concept makes it easier to test if forested areas generate less surface runoff than grasslands. The new implementation of VIC simplifies using knowledge of geospatial properties (e.g., soils data) and hydrological processes (e.g., expected fluxes for specific GRUs) to constrain model parameter values. Similarly, the GRU concepts simplify regularization across large geographical domains.

6- Avoid unrealistic combinations of land cover, soil and elevation zone. Unlike the traditional VIC configuration, the proposed VIV-GRU approach avoids unrealistic configuration of land cover, soil and elevation zones. An example is presented in Figure-2. This setup is with two elevation zones partitioned at the tree line and two land cover types, forest below tree line and bare soil above the tree line. The traditional VIC configuration assumes four different combinations, including the unrealistic case of forest above the tree line. This issue is avoided in vector-based setup of VIC-GRU as the set up will only include two GRUs with forest for lower elevation and with bare soil for higher elevation.

7- Possibility to incorporate additional data. If needed, additional data such as slope and aspect can be incorporated into the GRUs, accounting for changes in shortwave radiation or lapse rates for temperature. These additional controls can be implemented outside of the model in the forcing files. GRUs can be built also based on variation of leaf area index (LAI) giving an additional layer of information in addition to the land cover type.

8- Easier comparison of model simulations and in situ point-scale observation and visualization: The GRU implementation makes it easier to compare the point measurement to model simulation as the model simulations preserve extent of geospatial features. The GRU implementation also simplifies the comparison across GRUs; this comparison is very difficult in the typical VIC implementation because of the need to upscale geophysical information to the grid scale.

https://doi.org/10.5194/hess-2020-111
Preprint. Discussion started: 25 March 2020

9- Modular and controlled selection of models: The GRU implementation identifies the characteristics and spatial boundary of geospatial domains. A model might not be suitable for processes of some of the geospatial domains. Alternatively, processes of a GRU that is beyond the capacity of one model can be replaced with an alternative model. For example glaciers, can be replaced with more suitable models while the configuration and forcings remain identical. Consequently, the effect of features such as glacier can be better studied at larger scale hydrological cycle as more expert models can be applied to glacier while the rest of the GRUs can be simulated with a model that includes general processes.

2.3 Structural changes in VIC-GRU

We implemented several changes to the VIC process equations:

1- The VIC model uses the ARNO formulation, or its Nijssen representation, to represent baseflow (Todini et al., 1996, Nijssen et al., 2001). In this study we simplify the VIC baseflow formulation to a linear reservoir with one parameter, K_{slow}.

2- Preferential flow pathways are added to the VIC model by partitioning the runoff (fast reacting component of the VIC model) into (1) an effective surface flow component; and (2) recharge to the baseflow reservoir (interpreted as macropore flow). This partitioning is parameterized based on the macropore fraction (for further reading on the implementation refer to Gharari et al., 2019).

3- It is assumed that vegetation roots are restricted to the first two layers of the soil. This is due to the simplification of the VIC baseflow formulation.

2.4 mizuRoute, a vector-based routing scheme

In this study, we use the vector-based routing model mizuRoute (Mizukami et al., 2016). Vector-based routing models can be configured for separate computational units than the land model (e.g., configuring routing models using sub-basins derived from existing hydrologically conditioned DEMs such as Hydrosheds, Lehner et al., 2006, or Merit Hydro, Yamazaki et al., 2019). This removes the dependency of the routing to the grid size or GRUs configurations, and eliminates the decisions that are often made to represent routing-related parameters at grid scale. Therefore we

https://doi.org/10.5194/hess-2020-111
Preprint. Discussion started: 25 March 2020

Hydrology and Earth System Sciences
Open Access
Discussions

can ensure that two model configurations with different geospatial configurations are routed using the same routing configuration. The intersection between the computational units in the land model and the sub-basins in the routing model defines the contribution of each computational units in the land model to each river segment.

3 Data and methods

3.1 Experimental design

In this study, we configure the VIC model in a flexible vector-based framework to understand how model simulations depend on the spatial configuration. We consider four different methods to discretize the landscape for seven different spatial forcing grids (see Table 1). The landscape discretization methods include (1) simplified land cover and soils; (2) full detail for land cover and soils; (3) full detail for land cover and soils, including elevation zones; and (4) full detail for land cover and soils, including elevation zones and slope and aspect. The different spatial forcing grids are 4-km, 0.0625°, 0.125°, 0.25°, 0.5°, 1°, and 2°. This design enables us to separate our method to discretize the landscape from the spatial resolution of the forcing data.

Experiments are performed for the Bow River at Banff with a basin area of approximately 2210 km^2. The Bow River is located in the Canadian Rockies in the headwaters of the Saskatchewan River Basin. Most of the Bow River streamflow is due to snow melt (Nivo-glacial regime). The average basin elevation is 2130 m ranging from 3420 m at the peak top to 1380 m above mean sea level at the outlet (town of Banff). The basin annual precipitation is approximately 1000 mm with range of 500 mm for the Bow Valley up to 2000 mm for the mountain peaks. The predominant land cover is conifer forest in the Bow Valley and bare soil and rocks for mountain peaks above the tree line.

We design three experiments:

3.1.1 Experiment-1: How does the spatial configuration affect model performance?

As the first experiment, we focus on how well the various configurations simulate observed streamflow at the Bow River at Banff. We calibrate the parameters for the different configurations in Table 1. Model calibration is accomplished using the Genetic Algorithm implemented in the

https://doi.org/10.5194/hess-2020-111
Preprint. Discussion started: 25 March 2020

OSTRCIH framework (Mattot, 2005; Yoon and Shoemaker, 2001), maximizing the Nash-Sutcliffe Efficiency (E_{NS}, Nash and Sutcliffe 1970) using a total budget of 1000 model evaluations given the available resources limited by the most computationally expensive model (Case-4-4km).

3.1.2 Experiment-2: How well do calibrated parameter sets transfer across different model configurations?

As the second experiment, we focus on how various configurations can reproduce the result from the configuration with highest computational units for a given parameter set. In other words, this experiment evaluates accuracy-efficiency tradeoffs – i.e., the extent to which spatial simplifications affect model performance under the assumption that similar GRUs possess identical parameters across various configurations. This is important as it enables modelers to understand efficiency-accuracy tradeoffs, given the available data and the purpose of the modelling application. This experiment is based on perfect model experiments using the model with the highest computational unit as synthetic case (Case-4-4km). Synthetic streamflow for every river segment is generated using a calibrated parameter set for Case-4-4km-4km. The models with lower number of computational units are then simulated using the exact same parameter set used for generating the synthetic streamflow. The differences in streamflow simulation, quantified using E_{NS}, provide an understanding of how the simulations deteriorate when the spatial and forcing heterogeneities are masked or up-scaled. This also will bring an understanding on how sensitive the changes are along the river network and at the gauge location at which the models are calibrated against the observed streamflow data. Similarly, we compare the spatial patterns of snow water equivalent for the different spatial configurations.

3.1.3 Experiment 3: How do different model structures affect model performance?

As the third experiment, we focus on the effect of model structure on the performance metric (E_{NS}). This experiment, although not directly linked to the exploration of spatial configuration, is designed to investigate the effect of model structure changes on model performance which may affect our perception of parameter allocation across the GRUs (non-uniqueness of models, processes and parameter values)... For Case-2-4km, we calibrate the model with macropores activated and micropore deactivated. We call this model Case-2-4km-macro. We compare the

https://doi.org/10.5194/hess-2020-111
Preprint. Discussion started: 25 March 2020

Hydrology and Earth System Sciences
Open Access
Discussions

general model behavior looking into surface runoff and base-flow proportions of the streamflow for GRUs for the two model setups, Case-2-4km and Case-2-4km-macro.

3.2 Geospatial data and meteorological forcing

The inputs and forcing we used to set up the models are as follows:

1- Land cover: We used the land cover map NALCM-2005 v2 that is produced by CEC (Latifovic et al., 2004). NALCM-2005 v2 includes 19 different classes. The land cover map is used to set up the vegetation file and vegetation library (look up table) for the VIC model (Nijssen et al., 2001).

2- Soil texture: We used the Harmonized World Soil Data, HWSD (Fischer et al., 2008). For each polygon of the world harmonized soil we use the highest proportion of soil type. The HWSD provide the information for two soil layers, in this study we base our analyses on the lower soil layer reported in HWSD to define the soil characteristics needed for the VIC soil file.

3- Digital Elevation Model: in this study we make use of existing hydrologically conditioned digital elevation models to (1) derive the river network topology for the vector-based routing, mizuRoute and (2) to derive the slope, aspect and elevation zones which are used to estimate the forcing variables. For the first purpose we use hydrologically condition DEM of HydroSHED with resolution of 3 arc-second, approximately 90 meters; for the second purpose we use HydroSHED 15 arc-second DEM (approximately 500 meters).

4- Meteorological forcing: we used the WRF data set with the temporal resolution of 1 hour and spatial resolution of 4 km (Rasmussen and Liu, 2017). For upscaling the WRF input forcing, we use the CANDEX package (DOI: 10.5281/zenodo.2628351) to map the 7 forcing variables to various resolutions (1/16˚, 1/8˚, 1/4˚, 1/2˚, 1˚ and 2˚ from the original resolution of 4 km). We used the required variables from the WRF data set namely, total precipitation, temperature, short and long wave radiation at the ground surface, V, U components of wind speed and water vapor mixing ratio.

The shortwave radiation is rescaled based on the slope and aspect of the respective GRUs (refer to Appendix-A for more details). In this study we differentiated four aspects and five slope classes.

The temperature at 2 meters are adjusted using the environmental lapse rate for temperature of 6.5 km per 1000 meters. The assumed lapse rate aligns with earlier findings from the region of study (Pigeon and Jiskoot, 2008).

3.3 Observed data for model calibration

The daily streamflow is extracted from the HYDAT (WSC, Water Survey Canada) for Bow at Banff with gauges ID of 05BB001. This data is used for parameter calibration/identification of VIC-GRU parameter values.

3.4 Model parameters

3.4.1 VIC-GRU parameters

In the experiments for this study, we calibrate a subset of VIC parameters namely b_{inf}, E_{exp}, K_{sat}, $d_{2,\mathrm{forested}}$, $d_{2,\mathrm{non\text{-}forested}}$ and K_{slow} and $D_{\mathrm{macro\text{-}fract}}$ (names are mentioned in Table-2). We make sure that the $d_{2,\ \mathrm{forested}}$ is larger than the $d_{2,\mathrm{non\text{-}forested}}$ as the root depth are deeper for forested regions (constraining relative parameters).

3.4.2 MizuRoute parameters:

Impulse Response Function (IRF) routing method (Mizukami et al., 2016) is used for this study. IRF, which is derived based on diffusive wave equation, includes two parameters – wave velocity and diffusivity. The parameters for the routing scheme and river network topology for the mizuRoute is identical for all the configurations and experiments. The river network topology, assuming 100 km^2 starting threshold for the sub-basin size, is based on a 92-segment river network depicted in Figure-3d. The diffusive wave parameters are set to 1 m/s and 1000 m^2/s respectively and remain identical for all the river segments.

4 Results

4.1 Experiment-1

The various model configurations are compared with respect to the Nash-Sutcliffe performance metric (E_{NS}). Results show that all the models, including the ones that are configured with coarser resolution forcings, can simulate streamflow with E_{NS} as high as 0.70 (Table-3). These results indicate that the coarse resolution forcing input and lower computational units are able to yield equivalent E_{NS} of 0.7 and higher.

Although the performance metric of the various configurations, it is noteworthy to mention that the configuration of Case-4-0.5˚ has higher E_{NS} value compared to the cases with highest computational units, Case-4-4km for example. This might be due to various reasons including: (1) compensation of forcing aggregation on possible forcing bias at finer resolution; (2) compensation of forcing aggregation on model states and fluxes and possible adjustment for model structural inadequacy and hence directing the optimization algorithm to different possible solutions across configurations.

The model simulations, with E_{NS} higher than 0.7 for example, have very different soil parameters configuration. As an example, saturated hydraulic conductivity, K_{sat}, and slope of water retention curve, E_{exp}, can have very different combinations of values within the specified ranges for the parameters. Figure-4 illustrates the possible combinations of K_{sat} and E_{exp} with performance higher than E_{NS} greater than 0.7 for Case-2-4km. The result indicates the two parameters that are often fixed or a priori allocated based on look up tables can exhibit significant uncertainty and non-identifiability. Moreover, calibrating the VIC model using a sum-of-squared objective function at the basin outlet does not constrain the VIC soil parameters.

4.2 Experiment-2

The second experiment compares the performance of a parameter set with E_{NS} of above 0.7 from the Case-4-4km across the configurations with degraded geophysical information and aggregated spatial information. Figure-5 shows the evaluation metric, E_{NS}, for the streamflow of every river segment across the domain in comparison with the synthetic case (Case-4-4km). From Figure-5, it is clear that the E_{NS} is less sensitive for river segments with larger upstream area (read more downstream). This result has two major interpretations (*i*) the parameter transferability across various configuration is dependent on the sensitivity of simulation at the scale of interest and (*ii*) often inferred parameters at larger scale may not guarantee good performing parameters at the smaller scales.

Figure-6 shows the performance of the streamflow across various configurations for the most downstream river segment (the gauged river segment which is often used for parameter inference through calibration). Figure 6 illustrates that most of the configurations have similar scaled E_{NS} at the basin outlet. This analysis can be repeated for different parameter sets, e.g., poorly performing parameter sets or randomly selected parameter sets, to better understand accuracy-efficiency tradeoffs. Such analyses can provide insights on the appropriate model configurations for different applications. As an example, if model configurations of different complexity are known to show similar performance for a given parameter set, uncertainty and sensitivity analysis can be done initially on the models with fewer computational units and the results of the analysis can be applied to models with a higher number of computational units. This is however under assumption that parameters are transferable based on the concept of GRU.

To understand the spatial patterns of model simulations for all the configurations, we evaluate the distribution of the snow water equivalent, SWE, for the computational units on 5th of May 2004 (Figure-7). In general, the SWE follows the forcing resolution and its aggregation. Although coarser forcing resolutions results in coarser SWE simulation, the geospatial details such as elevation zones and slope and aspects result in more realistic representation of SWE as the snow layer is thinner for south facing slopes where more melt can be expected to occur, and thicker for higher elevation zones (compare SWE simulations for Case-4-2˚ and Case-3-2˚ in Figure-7) which is consistent with higher precipitation volumes and slower melt at higher elevation. Another observation from Figure-7 is the unrealistic distribution of SWE for configurations without elevation zones (Case-2 and Case-1). The lack of elevation zones results in both valley bottom and mountain tops to be forced with the same temperature. Snow is more durable in the forested areas as the result of model formulation, which are at lower elevation, while SWE is less for higher mountains, which is unrealistic.

We compared the maximum snow water equivalent across different configurations for a computational unit located in the Bow Valley Bottom (an arbitrary location of -116.134˚W and 51.382˚E) for the year 2004. Figure-8 illustrated the maximum snow water equivalent for the period of simulation. The result indicates that the SWE is higher for configurations with coarser forcing resolutions (almost double). This is due to the reduced temperature as a result of masking warmer valley bottom by cooler and higher forcing grids over the Rockies.

https://doi.org/10.5194/hess-2020-111
Preprint. Discussion started: 25 March 2020

4.3 Experiment-3

The calibration of model Case-2-4km and Case-2-4km-macro result in similar E_{NS} values of 0.78 and 0.75, indicating that both models are able to reproduce the observed streamflow to a similar extent although they are structurally different (the slow reservoir is recharged through only micropore and only macropore water movement in Case-2-4km and Case-2-4km-macro respectively). Figure-9 shows the streamflow hydrographs for the best performing parameter sets. . Observed Bow River at Banff has a minimum streamflow of approximately 15 cubic meter per second during snow accumulation months. This flow may be the result of regulation, return flow from human activities or unaccounted processes such as groundwater flow which are rather difficult for the linear reservoir of baseflow to simulate. Results (not shown) also indicate that both models structures generate 4 to 5 times more baseflow than surface runoff. This might be very intuitive as the model structure and parameters only have one processes, the slow reacting component, to simulate the long memory of this Nivo-glacial system and its annual cycle. Even though the two models are structurally different, both produce flow volumes through the surface and baseflow pathways that are consistent with streamflow observation. Similar to the uncertainty of model parameters, this result also shows the uncertainty of model structure and the fact that inclusion or exclusion of macropore water movement in the region of study and the context of modeling, may not change the overall results and similarly that these processes, micropore or macropore flow, cannot be inferred from the streamflow observation only.

5 Discussion

In this study, we proposed a vector-based configuration for land models and applied this setup to the VIC model. We used a vector-based routing scheme, mizuRoute, which was forced using output from the land model (one-way coupling). We term this new modelling approach VIC-GRU. Unlike the grid-based approach, there is no upscaling of land cover percentage or soil characteristics to a new grid size. This enables us to separate the effects of changes in forcing from changes in the spatial configurations. The vector-based setup also provides us with more flexibility in comparing the model simulations across GRUs, and also comparing model simulations with point measurements, such as snow water equivalent.

Our results illustrate that the VIC-GRU approach generates similar large-scale simulations of streamflow across the various spatial configurations when VIC-GRU is calibrated by maximizing the Nash-Sutcliffe score at the basin outlet. Similarly, we have shown that the VIC soil parameters can be very different when calibrated using different spatial configurations and that parameter transferability to different forcing resolutions and model setups is limited. This uncertainty is not often evaluated or reported for land models (Demaria et al., 2007) or is ignored by tying parameters, linking specific hydraulic conductivity to the slope of water retention curve, for example, so that the possible combination of them are reduced.

Land models are often applied at large spatial scales. The results clearly show that the deviation of streamflow is much lower in river segments with larger upstream area (Figure 5 and 6). It is often the case that the model parameters are inferred based on calibration on the streamflow at the basin outlet or over a large contributing area. We argue that this may not be a valid strategy for process understanding at the GRU scale, given the large uncertainty exhibited by the parameters. Therefore, hyper-resolution modeling efforts, Wood et al. 2011, may suffer from poor process representation and parameter identification at the scale of interest (Beven et al., 2015). What is needed instead of efficiency metrics that aggregate model behavior across both space (e.g. at the outlet of the larger catchment) and time (e.g. expressing the mismatch between observations and simulations across the entire observation period as a single number), is diagnostic evaluation of the model's process fidelity at the scale at which simulations are generated (e.g. Gupta et al., 2008; Clark et al., 2016).

We have shown that changes in model structure can result in identical performance for system-scale evaluation metrics (in this case, the Nash Sutcliffe Efficiency). We have changed the land model structure by replacing the micropore with macropore water movement to the slow reservoir. Similar to the parameter uncertainty, this indicates that lack or inclusion of macropore processes at the GRU scale does not have any notable effect on the efficiency score of the model simulation of streamflow at the outlet of the basin, even though the process simulations at the GRUs are different. Alternatively, this also shows that the micropore and macropore processes and their parameters may not be identifiable through calibration on the observed streamflow, which supports the argument against assuming that fine-scale parameters and processes can be inferred from large-scale observations. Although in this study we only focus on the processes and parameters that are often used to calibrate for the VIC model such as subsurface processes, it is possible to repeat the same analysis on wider range of processes such as snow processes or routing parameters.

It is often computationally expensive to evaluate the uncertainty and sensitivity of land models. Following the results presented in Figure-6, one can assume a configuration with fewer computational units can be a surrogate for a model with more computational units, under the condition that both models are known to behave similarly for a given parameter set. The calibration can be done on the model configuration with less computational unit and the parameters can be transferred directly to the model with more computational units, or can be used as an initial point for optimization algorithm to speed up the calibration process. Similarly the sensitivity analyses can be done primarily on the model with less computational units.

One might argue that the spatial discretization is important for realism of model fluxes and states. Moving to significantly high number of GRUs may result in computational units that are similar in their forcing and spatial variability. Based on the result of this study for snow water equivalent (Figure-8), we can argue that the snow patterns are fairly similar for the configurations that have elevation zones and finer resolution of forcing (case3 and 4 and forcing resolution less than 0.125 degree). It can be further explored if the model simulation at finer resolutions can be approximated by interpolating result of a model with coarser resolution ($m(\bar{x}|\theta) \sim \overline{m(x|\theta)}$, in which m is the model, x is forcing and $\boldsymbol{\theta}$ is the parameter set).

In this study and following the concept of GRUs, Grouped Response Units, we assumed the physical characteristics of soil and vegetation are identical for a given GRU across various model configurations. Techniques such as multiscale parameter regionalization (MPR, Samaniego et al., 2010) can be used to scale parameter values for different model configurations. However, applying these techniques, such as in this case that has significant parameter and process uncertainty and significance accuracy-performance tradeoff, should be put through rigorous tests (Merz et al., 2020, Liu et al., 2016).

Also, the degree of validity of the concept of GRU, hydrological similarity basd on physical attribute similarities, is debatable. For example, at the catchment scale, Oudin et al. (2010) have shown that the overlap between catchments with similar physiographic attributes and catchments with similar model performance for a given parameter set is only 60%. Physiographic similarity

https://doi.org/10.5194/hess-2020-111
Preprint. Discussion started: 25 March 2020

(in our case expressed through GRUs) does thus not necessarily imply similarity of hydrologic behavior, even though this is the critical assumption underlying GRUs. Although the GRUs in this study include slope and aspect, these characteristics were not translated into the model parameters and was only used for forcing manipulation. The VIC parameters can be linked to many more characteristics such as slope, height above nearest drainage (HAND, Renno et al., 2008), or Topographical Wetness Index (Beven and Kirkby, 1979) as has been done by Mizukami et al. (2017) and Cheney et al. (2018). However the functions that are used to linked the attribute to model characteristics remains mostly assumptions rather than inference and reproducibility of them are not very well explored (if possible).

In this study, the vector-based routing configuration does not include lakes and reservoirs. This is often a neglected element of land modeling efforts and has only attracted limited attention compared to the its impact on terrestrial water cycle (Haddeland et al., 2006, Yassin et al., 2018). The presence of lakes and reservoirs and their interconnections reduces the, already limited, ability of inference of land model parameter based on calibration on the observed streamflow because streamflow variability is reduced.

Although not primary the result of this study, however, the Nivo-glacial regime of the Bow River Basins is mostly dominated by snow melt that contributes to streamflow through baseflow (slow component of the hydrograph). The high Nash-Sutcliffe Efficiency, E_{NS}, is partly due to the fact that it is rather easy for the land model to capture the yearly cycle of the streamflow only with snow processes while rapid subsurface water movement, such as macropore, are largely missing in the land models but do not lead to notably increased efficiency scores when they are included in the model structure. More caution is needed for use of the land model for flood forecasting (Vionnet et al., 2019) for this region and all the Nivo-glacial river systems in western Canada, McKenzie, Yukon and Colombia River Basins.

6 Conclusions

The vector-based setup for the land model can provide modelers with more flexibility, e.g. impact of various forcing resolution or geospatial data representation, while avoiding decisions that are often taken for model configuration at grid level. The conclusion and messages from this study can be summarized as follows:

https://doi.org/10.5194/hess-2020-111
Preprint. Discussion started: 25 March 2020

Hydrology and Earth System Sciences Discussions

1) Regardless of observations at the scale of modeling, a model configuration with lower computational units, coarser resolution and less geospatial information, can produce model simulations with similar efficiency scores as configurations with higher computational units. The choice of model set up should be tested within the context and purpose of modeling for every different case.

2) The model with the highest number of computational units may not result in improved performance and better spatial simulation, in terms of obtained efficiency scores, and parameters can be transferred without substantial performance changes between certain model setups. Less computationally expensive configurations can be used instead for primary uncertainty and sensitivity analysis.

3) There is significant parameter and structural uncertainty associated with the VIC-GRU model. This uncertainty creates challenges for the process and parameter inference using calibration on streamflow. Any regionalization for parameters of the model should take into account these significant uncertainties. Our results recommend caution and more attention to the topic of parameter and process inference at finer modelling scales.

We also encourage the need for tools which can facilitate easier and more flexible set up of land models that in turn can facilitate the above mentioned research questions.

Acknowledgment. This research was undertaken thanks in part to funding from the Canada First Research Excellence Fund.

Data availability. All the data used in this study are available publicly (refer to references).

7 Appendix

7.1 Appendix – A

This appendix reflect on the methods and equations that have been used to calculate the ration of the solar radiation to flat surface and a surface with slope and aspect.

Declination angle: declination angle can be calculated for each day of year and is the same for the entire Earth based on (Ioan Sarbu, Calin Sebarchievici, in Solar Heating and Cooling Systems, 2017):

https://doi.org/10.5194/hess-2020-111
Preprint. Discussion started: 25 March 2020

Hydrology and Earth System Sciences Discussions

$$\delta = 23.45\frac{\pi}{180}\sin\left[\frac{2\pi}{360}\frac{360}{365}(284+N)\right] \tag{A-1}$$

In which N is the number of day in a year starting from beginning 1st of January.

Hour angle: is the angle expressed the solar hour. The reference of solar hour angle is solar noon (hour angle is set to zero) when the sun is passing the meridian of the observer or when the solar azimuth is 180. The hour angle can be calculated based on the:

$$\sin\omega = \frac{\sin\alpha - \sin\delta\sin\emptyset}{\cos\delta\cos\emptyset} \tag{A-2}$$

In which α, ϕ and δ are the altitude angle, latitude of the observer and inclination angle.

The solar noon is not exactly coinciding with12 am of the local time zone. However in this study we assume the two property are coinciding. The sunset and sunrise hour can be calculated from:

$$\cos\omega_s = -\tan\emptyset\tan\delta \tag{A-3}$$

For beyond 66.55 degree if the value of the right hand side is above 1 then there is 24 hour of daylight and if the right hand side is less than 1 the will be 24 hour of darkness.

The number of daylight hours that can be split before and after the solar noon equally can be calculated based on (assuming 15 degree for every 1 hour):

$$n = \frac{2\omega_s}{15}\frac{180}{\pi} \tag{A-4}$$

Altitude angle: is the angle of sun with the observer. This angle is maximum at solar noon and 0 for subset and sunrise. The altitude angle can be calculated based on the:

$$\sin\alpha = \sin\delta\sin\emptyset + \cos\delta\cos\omega\cos\emptyset \tag{A-5}$$

For the solar noon when ω, hour angle, is zero the question simplifies to:

$$\sin\alpha = \sin\delta\sin\emptyset + \cos\delta\cos\emptyset = \cos(\emptyset-\delta) = \sin\left(\frac{\pi}{2}-\emptyset+\delta\right) \tag{A-6}$$

This result the altitude angle for the solar noon to be:

https://doi.org/10.5194/hess-2020-111
Preprint. Discussion started: 25 March 2020

Hydrology and Earth System Sciences Discussions

$$\alpha = \frac{\pi}{2} - \emptyset + \delta \quad \text{(A-7)}$$

Solar Azimuth: The solar azimuth angle, θ_{Sun} reflect on the angle of the sun on the sky from the North with clockwise rule. The azimuth angle can be calculated as:

$$\sin\theta_{Sun} = \frac{\sin\omega\cos\delta}{\cos\alpha} \quad \text{(A-8)}$$

The solar azimuth angle for the solar noon is set to be 180 degree (calculated clockwise from north direction).

The azimuth at the sunset and sunrise can be calculated using:

$$\sin\theta_{Sun,rise} = -\sin\omega_s\cos\delta \quad \text{(A-9)}$$

$$\sin\theta_{Sun,set} = \sin\omega_s\cos\delta \quad \text{(A-10)}$$

Surface Azimuth (a.k.a. aspect): The surface azimuth angle, $\theta_{Surface}$reflect the direction of the any tilted surface to the north direction. This azimuth is fixed for any point while the solar azimuth changes over hours and seasons.

Angle of incidence $\boldsymbol{\theta}$: this angle represent the angle between a sloped surface and the sun rays that reaches this sloped surface. The model angle of the incidence for a slope surface β, and aspect of $\theta_{Surface}$ over latitude of $\emptyset$ can be calculated as (Kalogirou, in Solar Energy Engineering, 2009, in the reference formulation the Azimuth is from south which is corrected here for North):

$$\cos\theta = \sin\delta\sin\emptyset\cos\beta + \sin\delta\cos\emptyset\sin\beta\cos\theta_{Surface} + \cos\delta\cos\emptyset\cos\beta\cos\omega -$$
$$\cos\delta\sin\emptyset\sin\beta\cos\theta_{Surface}\cos\omega - \cos\delta\sin\beta\sin\theta_{Surface}\sin\omega \quad \text{(A-11)}$$

For the flat surface, both $\theta_{Surface}$ and β, is set to zero, the incident angle can be calculated for the flat surface as

$$\cos\theta_{flat} = \sin\delta\sin\emptyset + \cos\delta\cos\emptyset\cos\omega \quad \text{(A-12)}$$

In case where the angle of incident is larger than 90 degrees the surface shades itself.

Hydrology and Earth System Sciences
Open Access
EGU
Discussions

Amendment of short wave radiation based on slope and aspect. In this study we correct the WRF short wave radiation based on the surface slope and aspect. We first back calculated the incoming short wave radiation by dividing the provided short wave radiation by the cosine of the incident angle of the flat surface. Then we can calculate the solar radiation of the sloped surface multiplying this value to the cosine of the incident angle of the slope surface. Basically this ratio is:

$$R = \frac{\cos\theta}{\cos\theta_{flat}} \tag{A-13}$$

The effect of the atmosphere is considered in the WRF product itself. However, and for incident level close to 90 degrees the ratio, *R*, might be very high values which result in the surface receiving unrealistically high value of radiation even higher than the solar constant, 1366 W/m2, at the top of the atmosphere. For cases with cos values of incident angle lower than 0.05 we set the ratio to 0 to avoid this unrealistic condition.

8 References:

Annear, R.L. and Wells, S.A.: A comparison of five models for estimating clear-sky solar radiation. Water resources research, 43(10), 2007.

Beven, K., Cloke, H., Pappenberger, F., Lamb, R. and Hunter, N.: Hyperresolution information and hyperresolution ignorance in modelling the hydrology of the land surface. Science China Earth Sciences, 58(1), pp.25-35, 2015.

Beven, K.J. and Kirkby, M.J.: A physically based, variable contributing area model of basin hydrology/Un modèle à base physique de zone d'appel variable de l'hydrologie du bassin versant. Hydrological Sciences Journal, 24(1), pp.43-69, 1979.

Beven, K.J.: Rainfall-runoff modelling: the primer. John Wiley & Sons, 2011.

Blöschl, Günter, Rodger B. Grayson, and Murugesu Sivapalan: On the representative elementary area (REA) concept and its utility for distributed rainfall-runoff modelling. Hydrological Processes 9, no. 3-4 313-330, 1995.

https://doi.org/10.5194/hess-2020-111
Preprint. Discussion started: 25 March 2020

Chaney, N.W., Van Huijgevoort, M.H., Shevliakova, E., Malyshev, S., Milly, P.C., Gauthier, P.P. and Sulman, B.N.: Harnessing big data to rethink land heterogeneity in Earth system models. Hydrology and Earth System Sciences, 22(6), pp.3311-3330, 2018.

Clark, M.P., Nijssen, B., Lundquist, J.D., Kavetski, D., Rupp, D.E., Woods, R.A., Freer, J.E., Gutmann, E.D., Wood, A.W., Brekke, L.D. and Arnold, J.R.: The structure for unifying multiple modeling alternatives (SUMMA), Version 1.0: Technical description. NCAR Tech. Note NCAR/TN-5141STR, 2015.

Clark, M.P., Slater, A.G., Rupp, D.E., Woods, R.A., Vrugt, J.A., Gupta, H.V., Wagener, T. and Hay, L.E.: Framework for Understanding Structural Errors (FUSE): A modular framework to diagnose differences between hydrological models. Water Resources Research, 44(12), 2008.

Clark P. M., Marc FP Bierkens, Luis Samaniego, Ross A. Woods, Remko Uijlenhoet, Katrina E. Bennett, Valentijn Pauwels, Xitian Cai, Andrew W. Wood, and Christa D. Peters-Lidard. "The evolution of process-based hydrologic models: historical challenges and the collective quest for physical realism." Hydrology and Earth System Sciences (Online) 21, no. LA-UR-17-27603, 2016.

Demaria, E.M., Nijssen, B. and Wagener, T.: Monte Carlo sensitivity analysis of land surface parameters using the Variable Infiltration Capacity model. Journal of Geophysical Research: Atmospheres, 112(D11), 2007.

Desborough, C.E.: Surface energy balance complexity in GCM land surface models. Climate Dynamics, 15(5), pp.389-403, 1999.

Fenicia, F., Kavetski, D. and Savenije, H.H.: Elements of a flexible approach for conceptual hydrological modeling: 1. Motivation and theoretical development. Water Resources Research, 47(11), 2011.

Fischer, G., F. Nachtergaele, S. Prieler, H.T. van Velthuizen, L. Verelst, D. Wiberg: Global Agro-ecological Zones Assessment for Agriculture (GAEZ 2008). IIASA, Laxenburg, Austria and FAO, Rome, Italy, 2008.

https://doi.org/10.5194/hess-2020-111
Preprint. Discussion started: 25 March 2020

Flügel, W.A.: Delineating hydrological response units by geographical information system analyses for regional hydrological modelling using PRMS/MMS in the drainage basin of the River Bröl, Germany. Hydrological Processes, 9(3-4), pp.423-436, 1995.

Gharari, S., Clark, M., Mizukami, N., Wong, J.S., Pietroniro, A. and Wheater, H., 2019. Improving the representation of subsurface water movement in land models. Journal of Hydrometeorology, 2019.

Haddeland, I., Lettenmaier, D.P. and Skaugen, T.: Effects of irrigation on the water and energy balances of the Colorado and Mekong river basins. Journal of Hydrology, 324(1-4), pp.210-223, 2006.

Haddeland, I., Matheussen, B.V. and Lettenmaier, D.P., 2002. Influence of spatial resolution on simulated streamflow in a macroscale hydrologic model. Water Resources Research, 38(7), pp.29-1, 2002.

Hamman, J.J., Nijssen, B., Bohn, T.J., Gergel, D.R. and Mao, Y.: The Variable Infiltration Capacity model version 5 (VIC-5): infrastructure improvements for new applications and reproducibility. *Geoscientific Model Development (Online)*, *11*(8), 2018.

Hrachowitz, M. and Clark, M.P.: HESS Opinions: The complementary merits of competing modelling philosophies in hydrology. Hydrology and Earth System Sciences, 21(8), p.3953, 2017.

Jarvis, P.G.: The interpretation of the variations in leaf water potential and stomatal conductance found in canopies in the field. Philosophical Transactions of the Royal Society of London. B, Biological Sciences, 273(927), pp.593-610, 1976.

Kalogirou, S.: Solar Energy Engineering, edited by Soteris A. Kalogirou, 2009.

Kirkby, M. J. and Weyman, D. R: `Measurements of contributing area in very small drainage basins', Seminar Series B, No. 3. Department of Geography, University of Bristol, Bristol, 1974.

Knudsen, J., Thomsen, A. and Refsgaard, J.C.: WATBALA Semi-Distributed, Physically Based Hydrological Modelling System. Hydrology Research, 17(4-5), pp.347-362, 1986.

https://doi.org/10.5194/hess-2020-111
Preprint. Discussion started: 25 March 2020

Koster, Randal D., and Max J. Suarez: Modeling the land surface boundary in climate models as a composite of independent vegetation stands, Journal of Geophysical Research: Atmospheres 97, no. D3, 2697-2715, 1992.

Kouwen, N., Soulis, E.D., Pietroniro, A., Donald, J. and Harrington, R.A.: Grouped response units for distributed hydrologic modeling. Journal of Water Resources Planning and Management, 119(3), pp.289-305, 1993.

Latifovic, R., Zhu, Z., Cihlar, J., Giri, C., & Olthof, I.: Land cover mapping of North and Central America - Global Land Cover 2000. Remote Sensing of Environment, 89:116-127.

Lehner, B., Verdin, K. and Jarvis, A.: HydroSHEDS technical documentation, version 1.0. World Wildlife Fund US, Washington, DC, pp.1-27, 2006

Liang, X., Guo, J. and Leung, L.R.: Assessment of the effects of spatial resolutions on daily water flux simulations. Journal of Hydrology, 298(1-4), pp.287-310, 2004.

Liang, X., Lettenmaier, D.P., Wood, E.F. and Burges, S.J.: A simple hydrologically based model of land surface water and energy fluxes for general circulation models. Journal of Geophysical Research: Atmospheres, 99(D7), pp.14415-14428, 1994.

Liu, H., Tolson, B.A., Craig, J.R. and Shafii, M.: A priori discretization error metrics for distributed hydrologic modeling applications. *Journal of hydrology*, *543*, pp.873-891, 2016.

Manabe, Syukuro: Climate and the ocean circulation: I. The atmospheric circulation and the hydrology of the earth's surface. Monthly Weather Review 97, no. 11, 739-774, 1969.

Marsh, C.B., Pomeroy, J.W. and Spiteri, R.J.: Implications of mountain shading on calculating energy for snowmelt using unstructured triangular meshes. Hydrological Processes, 26(12), pp.1767-1778, 2012.

Matott, L.S.: OSTRICH: An optimization software tool: Documentation and users guide. University at Buffalo, Buffalo, NY, 2005.

Maxwell, R. M., L. E. Condon, and S. J. Kollet: A high-resolution simulation of groundwater and surface water over most of the continental US with the integrated hydrologic model ParFlow v3, Geoscientific model development 8, no. 3, 923, 2015.

Melsen, L., Teuling, A., Torfs, P., Zappa, M., Mizukami, N., Clark, M. and Uijlenhoet, R.: Representation of spatial and temporal variability in large-domain hydrological models: case study for a mesoscale pre-Alpine basin. Hydrology and Earth System Sciences, 20(6), pp.2207-2226, 2016.

Merz, R., Tarasova, L. and Basso, S.,: Parameter's controls of distributed catchment models–How much information is in conventional catchment descriptors?. *Water Resources Research*, p.e2019WR026008, 2020.

Mizukami, N., Clark, M.P., Sampson, K., Nijssen, B., Mao, Y., McMillan, H., Viger, R.J., Markstrom, S.L., Hay, L.E., Woods, R. and Arnold, J.R.: mizuRoute version 1: a river network routing tool for a continental domain water resources applications. Geoscientific Model Development, 9(6), pp.2223-2238, 2016.

Naef, F., Scherrer, S. and Weiler, M.: A process based assessment of the potential to reduce flood runoff by land use change. Journal of hydrology, 267(1-2), pp.74-79, 2002.

Newman, A.J., Clark, M.P., Winstral, A., Marks, D. and Seyfried, M.: The use of similarity concepts to represent subgrid variability in land surface models: Case study in a snowmelt-dominated watershed. Journal of Hydrometeorology, 15(5), pp.1717-1738, 2014.

Nijssen, B., O'Donnell, G.M., Hamlet, A.F. and Lettenmaier, D.P.: Hydrologic sensitivity of global rivers to climate change. Climatic change, 50(1-2), pp.143-175, 2001.

Niu, G.Y., Yang, Z.L., Dickinson, R.E. and Gulden, L.E.: A simple TOPMODEL-based runoff parameterization (SIMTOP) for use in global climate models. Journal of Geophysical Research: Atmospheres, 110(D21), 2005.

Niu, G.Y., Yang, Z.L., Mitchell, K.E., Chen, F., Ek, M.B., Barlage, M., Kumar, A., Manning, K., Niyogi, D., Rosero, E. and Tewari, M.: The community Noah land surface model with

https://doi.org/10.5194/hess-2020-111
Preprint. Discussion started: 25 March 2020

multiparameterization options (Noah-MP): 1. Model description and evaluation with local-scale measurements. Journal of Geophysical Research: Atmospheres, 116(D12), 2011.

Olivera, F., Valenzuela, M., Srinivasan, R., Choi, J., Cho, H., Koka, S. and Agrawal, A.: ARCGIS-SWAT: A GEODATA MODEL AND GIS INTERFACE FOR SWAT 1. JAWRA Journal of the American Water Resources Association, 42(2), pp.295-309, 2006.

Oudin, L., Kay, A., Andréassian, V. and Perrin, C.: Are seemingly physically similar catchments truly hydrologically similar?. Water Resources Research, 46(11), 2010.

Park, S.J. and Van De Giesen, N.: Soil–landscape delineation to define spatial sampling domains for hillslope hydrology. Journal of Hydrology, 295(1-4), pp.28-46, 2004.

Pietroniro, A., Fortin, V., Kouwen, N., Neal, C., Turcotte, R., Davison, B., Verseghy, D., Soulis, E.D., Caldwell, R., Evora, N. and Pellerin, P.: Development of the MESH modelling system for hydrological ensemble forecasting of the Laurentian Great Lakes at the regional scale. Hydrology and Earth System Sciences Discussions, 11(4), pp.1279-1294, 2007.

Pigeon, K.E. and Jiskoot, H.: Meteorological controls on snowpack formation and dynamics in the southern Canadian Rocky Mountains. Arctic, antarctic, and alpine research, 40(4), pp.716-730, 2008.

Pitman, A.J.: The evolution of, and revolution in, land surface schemes designed for climate models. International Journal of Climatology: A Journal of the Royal Meteorological Society, 23(5), pp.479-510, 2003.

Rasmussen, R., and C. Liu.: High Resolution WRF Simulations of the Current and Future Climate of North America. Research Data Archive at the National Center for Atmospheric Research, Computational and Information Systems Laboratory. https://doi.org/10.5065/D6V40SXP, 2017.

Reggiani, P., Hassanizadeh, S.M., Sivapalan, M. and Gray, W.G.: A unifying framework for watershed thermodynamics: constitutive relationships. Advances in Water Resources, 23(1), pp.15-39, 1999.

https://doi.org/10.5194/hess-2020-111
Preprint. Discussion started: 25 March 2020

Hydrology and Earth System Sciences Discussions

Rennó, C.D., Nobre, A.D., Cuartas, L.A., Soares, J.V., Hodnett, M.G., Tomasella, J. and Waterloo, M.J.: HAND, a new terrain descriptor using SRTM-DEM: Mapping terra-firme rainforest environments in Amazonia. Remote Sensing of Environment, 112(9), pp.3469-3481, 2008.

Samaniego, L., Kumar, R. and Attinger, S.: Multiscale parameter regionalization of a grid-based hydrologic model at the mesoscale. Water Resources Research, 46(5), 2010.

Samaniego, L., Kumar, R., Thober, S., Rakovec, O., Zink, M., Wanders, N., Eisner, S., Müller Schmied, H., Sutanudjaja, E., Warrach-Sagi, K. and Attinger, S.: Toward seamless hydrologic predictions across spatial scales. Hydrology and Earth System Sciences, 21(9), pp.4323-4346, 2017.

Sarbu, I. and Sebarchievici, C.: Thermal Energy Storage. Solar Heating and Cooling Systems, pp.99-138, 2017.

Savenije, H.H.G.: HESS Opinions" Topography driven conceptual modelling (FLEX-Topo)". Hydrology and Earth System Sciences, 14(12), pp.2681-2692, 2010.

Shafii, M., Basu, N., Craig, J.R., Schiff, S.L. and Van Cappellen, P.: A diagnostic approach to constraining flow partitioning in hydrologic models using a multiobjective optimization framework. Water Resources Research, 53(4), pp.3279-3301, 2017.

Shrestha, P., Sulis, M., Simmer, C. and Kollet, S.: Impacts of grid resolution on surface energy fluxes simulated with an integrated surface-groundwater flow model. Hydrology and Earth System Sciences, 19(10), pp.4317-4326, 2015.

Singh, R.S., Reager, J.T., Miller, N.L. and Famiglietti, J.S.: Toward hyper-resolution land-surface modeling: The effects of fine-scale topography and soil texture on CLM 4.0 simulations over the S outhwestern US. Water Resources Research, 51(4), pp.2648-2667, 2015.

Son, K. and Sivapalan, M.: Improving model structure and reducing parameter uncertainty in conceptual water balance models through the use of auxiliary data. Water resources research, 43(1), 2007.

https://doi.org/10.5194/hess-2020-111
Preprint. Discussion started: 25 March 2020

Troy, T.J., Wood, E.F. and Sheffield, J.: An efficient calibration method for continental-scale land surface modeling. Water Resources Research, 44(9), 2008.

Uhlenbrook, S., Roser, S. and Tilch, N.: Hydrological process representation at the meso-scale: the potential of a distributed, conceptual catchment model. Journal of Hydrology, 291(3-4), pp.278-296, 2004.

Vionnet, V., Fortin, V., Gaborit, E., Roy, G., Abrahamowicz, M., Gasset, N. and Pomeroy, J.W.: High-resolution hydrometeorological modelling of the June 2013 flood in southern Alberta, Canada. Hydrology and Earth System Sciences Discussions, pp.1-36, 2019.

Vivoni, Enrique R., Valeri Y. Ivanov, Rafael L. Bras, and Dara Entekhabi: Generation of triangulated irregular networks based on hydrological similarity, Journal of hydrologic engineering 9, no. 4, 288-302, 2004.

Winter, T.C.: The concept of hydrologic landscapes 1. JAWRA Journal of the American Water Resources Association, 37(2), pp.335-349, 2001.

Wood, E.F., Roundy, J.K., Troy, T.J., Van Beek, L.P.H., Bierkens, M.F., Blyth, E., de Roo, A., Döll, P., Ek, M., Famiglietti, J. and Gochis, D.: Hyperresolution global land surface modeling: Meeting a grand challenge for monitoring Earth's terrestrial water. Water Resources Research, 47(5), 2011.

Wood, E.F., Sivapalan, M., Beven, K. and Band, L.: Effects of spatial variability and scale with implications to hydrologic modeling. Journal of hydrology, 102(1-4), pp.29-47, 1988.

Yamazaki, D., Ikeshima, D., Sosa, J., Bates, P.D., Allen, G. and Pavelsky, T.: MERIT Hydro: A high-resolution global hydrography map based on latest topography datasets. Water Resources Research, 2019.

Yassin, F., Razavi, S., Elshamy, M., Davison, B., Sapriza-Azuri, G. and Wheater, H.: Representation and improved parameterization of reservoir operation in hydrological and land-surface models. Hydrology and Earth System Sciences, 23(9), pp.3735-3764, 2019.

https://doi.org/10.5194/hess-2020-111
Preprint. Discussion started: 25 March 2020

Yoon, J.-H.,Shoemaker, C. A.: Improved real-coded GA for groundwater bioremediation. Journal of Computing in Civil Engineering 15, 224-231, 2001.

Zhao, R.J.:. The xinanjiang model. In Proceedings of the Oxford Symposium, 1980.

9 Tables

Table – 1 the number of computational units for the Bow River at Banff, given different spatial discretization of land cover, soil type, elevation zones and slope and aspects forced with various forcing resolutions.

	Forcing resolution	**Case 4** 4 aspect groups; 5 slope groups; 19 classes of land cover; 500 meter elevation zones;	**Case 3** no aspect groups; no slope groups; 19 classes of land cover; 500 meter elevation zones;	**Case 2** no aspect groups; no slope groups; 19 classes of land cover; no elevation zones;	**Case 1** no aspect groups; no slope groups, 3 classes of land cover, one dominant soil type no elevation zones;
Number of GRUs	--	**582**	**65**	**56**	**3**
Number of Computational units (GRUs forced at various forcing resolutions)	4km	6631	1508	941	479
	0.0625	5224	1098	663	290
	0.125	3079	515	283	94
	0.25	2013	306	154	39
	0.5	1332	184	93	21
	1.0	917	116	56	12
	2.0	767	89	42	6

https://doi.org/10.5194/hess-2020-111
Preprint. Discussion started: 25 March 2020

Table-2 the VIC-GRU model parameters that are subjected to perturbation for model calibration for the designed experiments.

Parameter symbol	Parameter name	Minimum value	Maximum value	Unit	Explanation
b_{inf}	Variable infiltration parameter	0.01	0.50	[-]	
E_{exp}	The slope of water retention curve	3.00	12.00	[-]	
K_{sat}	Saturated hydraulic conductivity	5.00	1000.00	[mm/day]	Fixed at very low rate, 0.0001, for the macropore model in experiment 3 to diable micropore water movement to the slow reservoir.
d_1	The depth of top soil layer	0.2	0.2	m	Fixed at 20 cm for both forested and non-forested GRUs
$d_{2,forested}$	The depth of the second soil layer for forested GRUs	0.2	2	m	
$d_{2,non\text{-}forested}$	The depth of the second soil layer for non-forested GRUs	0.2	$d_{2,forested}$	m	The maximum is bounded by the $d_{2,forested}$
D_{root}	The distribution of root in the two soil layers.	0.5	*0.5*		Fixed at 50% for the top and lower soil layers.
K_{slow}	Slow reservoir coefficient	0.001	0.9	[1/day]	
$D_{macro\text{-}fract}$	Macropore fraction	0.0	1.0	[-]	Fixed at 0.00 for experiment 1 and experiment 2, varying for experiment 3.

https://doi.org/10.5194/hess-2020-111
Preprint. Discussion started: 25 March 2020

Hydrology and Earth System Sciences
Discussions

Table-3 – The E_{NS} for the different model configurations. Details on the geospatial cases are provided in Table 1.

Forcing resolution	**Case 4**	**Case 3**	**Case 2**	**Case 1**
4km	0.80	0.80	0.78	0.74
0.0625°	0.80	0.80	0.78	0.77
0.125°	0.80	0.80	0.76	0.73
0.25°	0.82	0.81	0.76	0.76
0.5°	0.84	0.84	0.76	0.75
1.0°	0.82	0.81	0.78	0.78
2.0°	0.78	0.78	0.72	0.76

https://doi.org/10.5194/hess-2020-111
Preprint. Discussion started: 25 March 2020

Hydrology and Earth System Sciences
Discussions

10 Figures

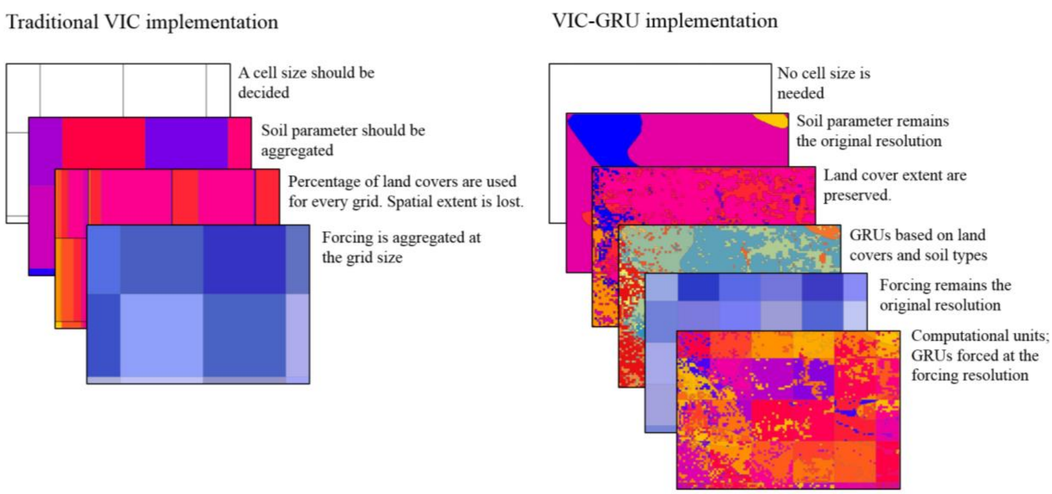

Figure-1- (a) Traditional VIC implementation and (b) new VIC implementation (VIC-GRU).

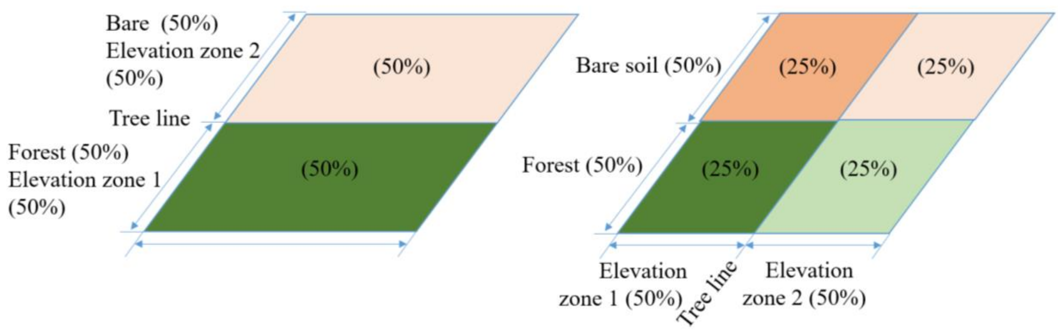

Figure-2 – (Left) the true configuration of a natural system with land cover consist of 50% Bare soil and 50% forest within a grid located in two different elevation zones above and below the tree line and (right) the traditional VIC configurations for the given system at the grid for the two elevation zones and 2 land cover which results in unrealistic combination of forest cover above the tree line and bare soil below the tree line.

https://doi.org/10.5194/hess-2020-111
Preprint. Discussion started: 25 March 2020

Hydrology and Earth System Sciences
Open Access
Discussions

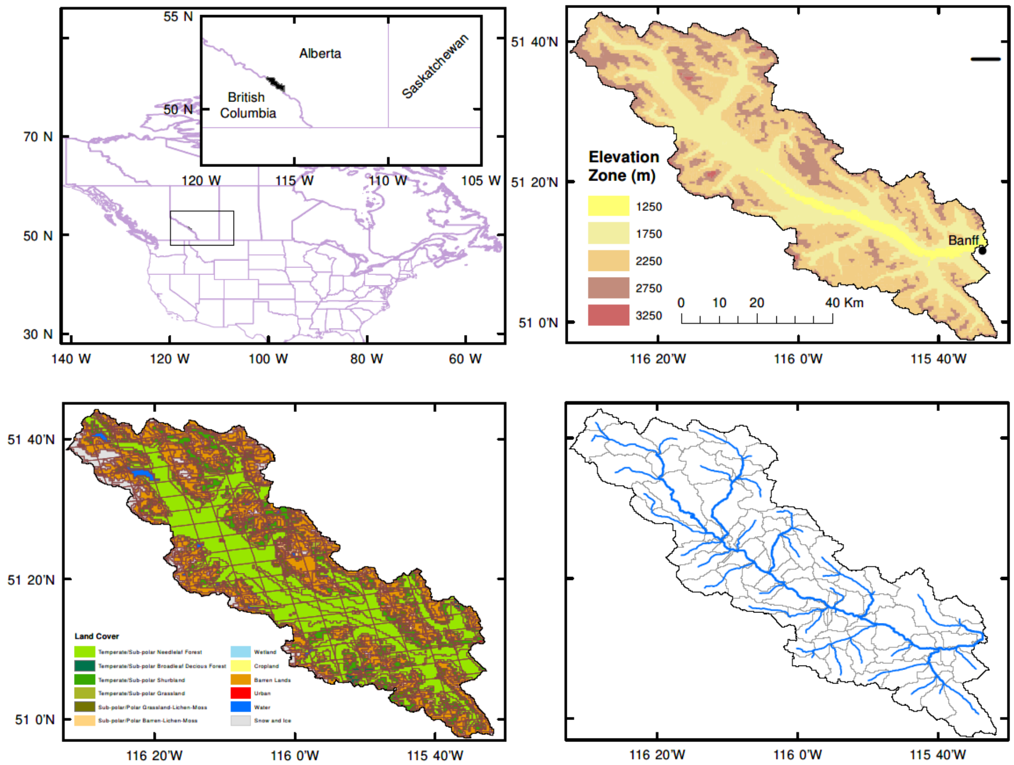

Figure – 3 (a) The location of the Bow River Basin to Banff (b) GRUs for Case-3 color-coded for elevation zones, (c) computational units for the Case-3-4km (Case-3 forced at forcing of 4 km resolutions) and (d) river network topology and associated sub-basins for the vector-based routing.

https://doi.org/10.5194/hess-2020-111
Preprint. Discussion started: 25 March 2020

Hydrology and Earth System Sciences Discussions

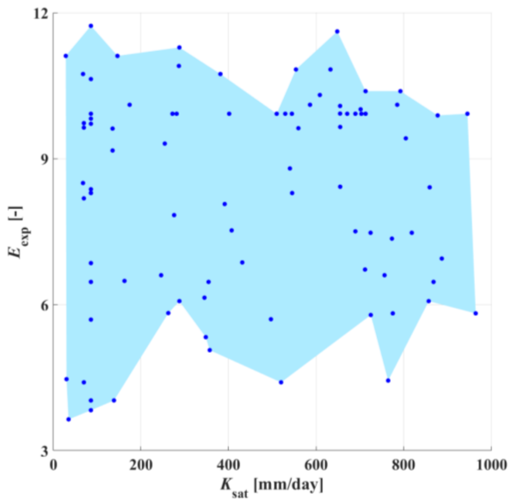

Figure-4 – The spread of two parameters, saturated hydraulic conductivity, K_{sat}, and slope of water retention curve, E_{exp}, for the parameters sets that have performance metric, E_{NS}, of more than 0.7 for configuration Case-2-4km. The axis are set to the ranges of the parameters.

https://doi.org/10.5194/hess-2020-111
Preprint. Discussion started: 25 March 2020

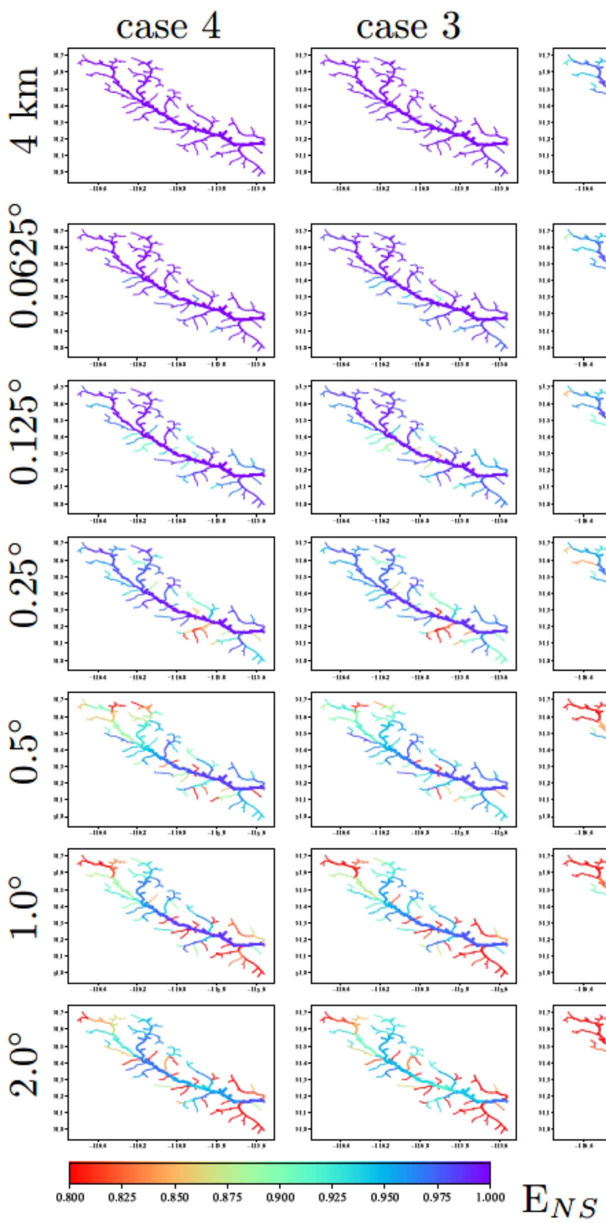

Figure 5 – Deviation of the simulated streamflow at river segments in comparison with the synthetic case of GRUs forced at 4km, Case-4-4km, expressed in performance metric, E_{NS}.

https://doi.org/10.5194/hess-2020-111
Preprint. Discussion started: 25 March 2020

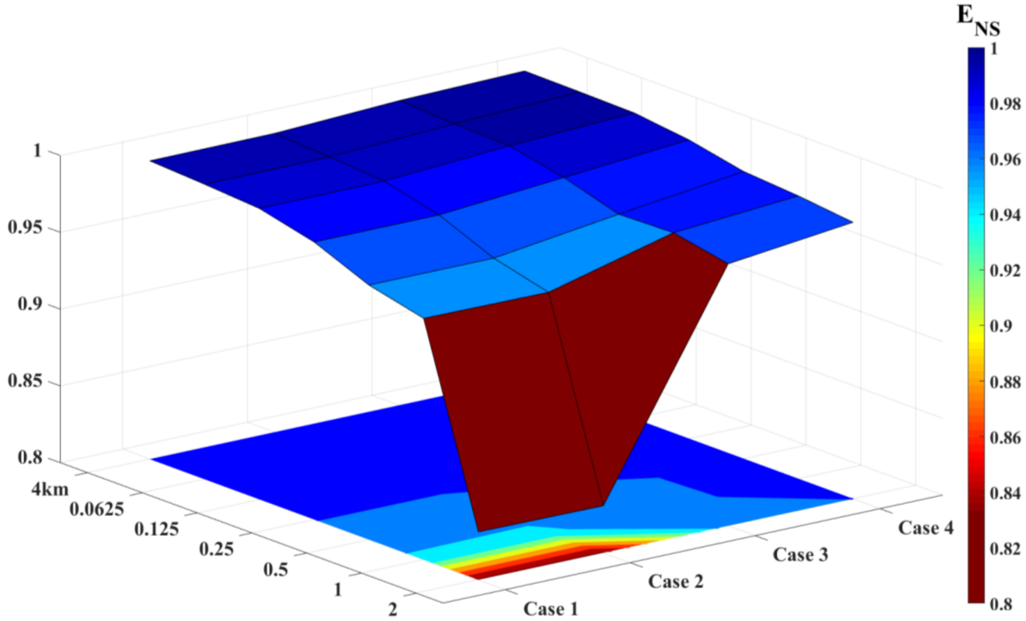

840

841 Figure -6- The relative performance of model simulation across various configurations with a
842 single parameter set.

843

https://doi.org/10.5194/hess-2020-111
Preprint. Discussion started: 25 March 2020

Hydrology and Earth System Sciences
Open Access
EGU
Discussions

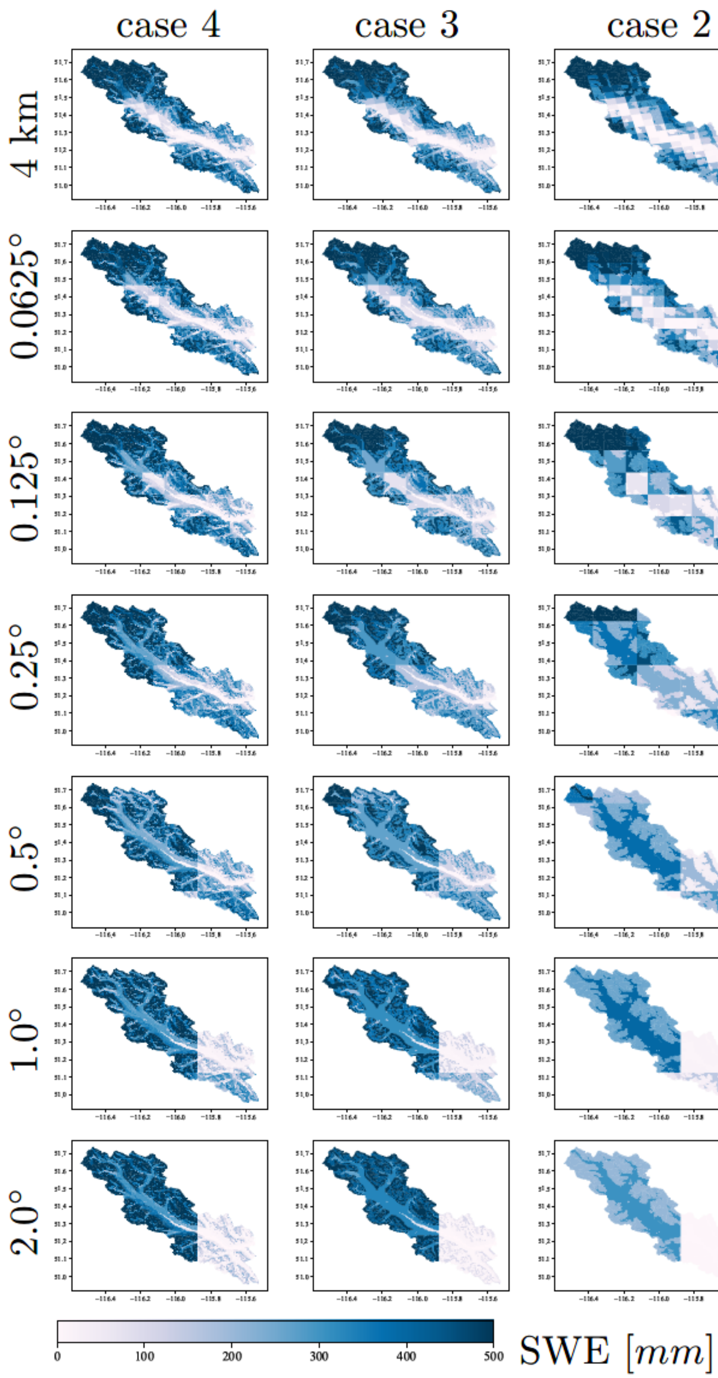

Figure 7- Comparison of the snow water equivalent for 5th of May 2004 for various configurations.

https://doi.org/10.5194/hess-2020-111
Preprint. Discussion started: 25 March 2020

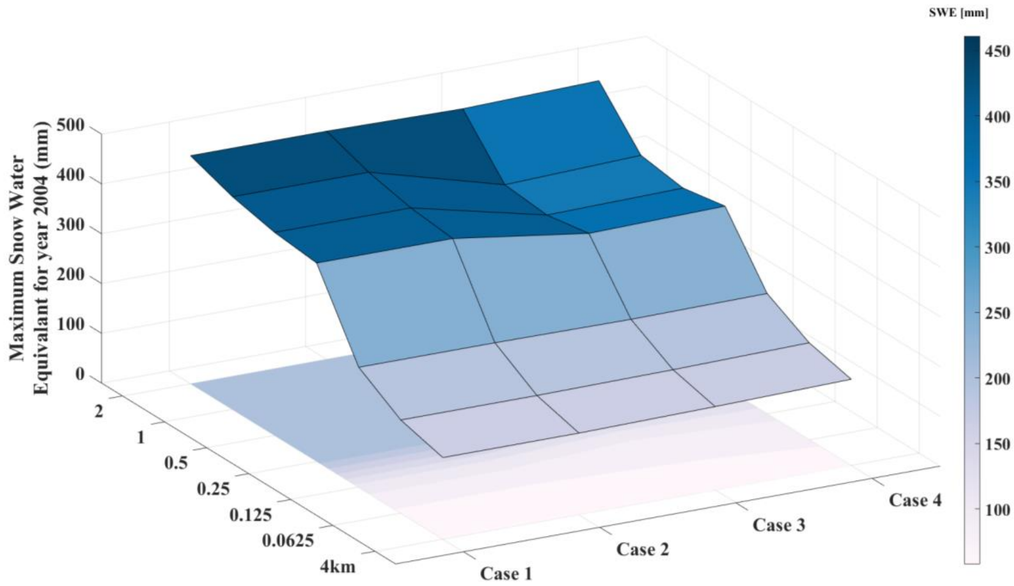

Figure-8- Maximum of snow water equivalent for an arbitrary location of -116.134˚W and 51.382˚E located in Bow Valley Bottom across various model configurations for the year 2004.

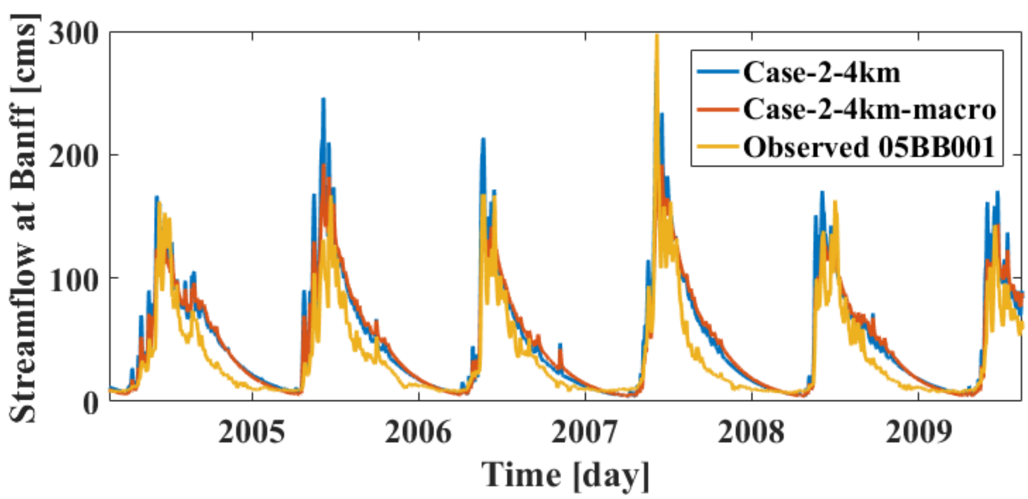

Figure-9 comparison between the streamflow observation for Bow at Banff (05BB001) and model with only micropore flow to slow reservoir, Case-2-4km, and only macropore to the slow reservoir, Case-2-4km-macro.

https://doi.org/10.5194/hess-2020-111
Preprint. Discussion started: 25 March 2020

Hydrology and Earth System Sciences Discussions
Open Access

854

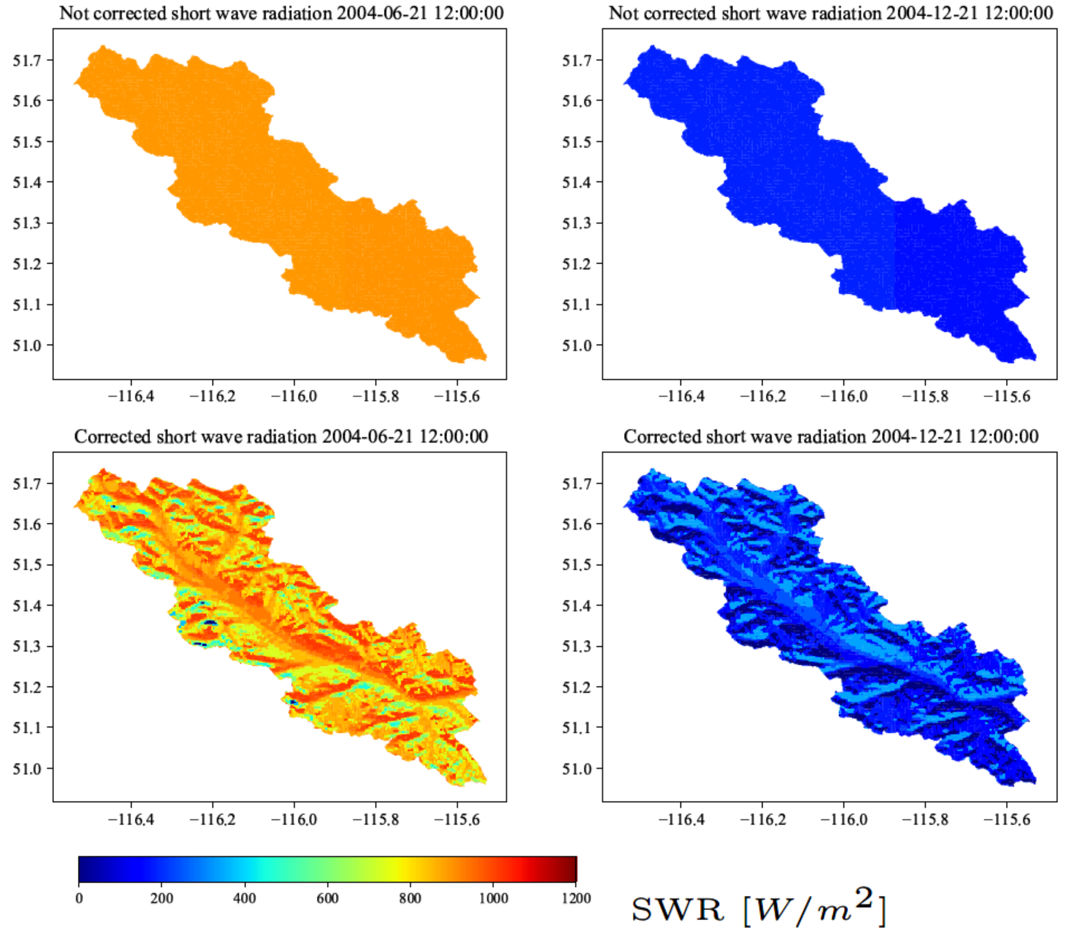

855

856 Figure A-1 Short wave radiation for (top left) not corrected for slope and aspect and (bottom left)
857 corrected for slope and aspect for 21st June 2020 and (top right) not corrected for slope and ascpet
858 and (bottom right) corrected for slope and aspect for 21st December 2020.

859